

Supplementary Material

Table S1. Fluid phase diffusivities values

$D_{f,NH3}$	$1.2 \cdot 10^{-9} T^{1.75}$
$D_{f,NO}$	$1.2 \cdot 10^{-9} T^{1.75}$
$D_{f,N2O}$	$0.8 \cdot 10^{-9} T^{1.75}$
$D_{f,N2}$	$1.3 \cdot 10^{-9} T^{1.75}$
$D_{f,NO2}$	$0.8 \cdot 10^{-9} T^{1.75}$
$D_{f,O2}$	$1.1 \cdot 10^{-9} T^{1.75}$

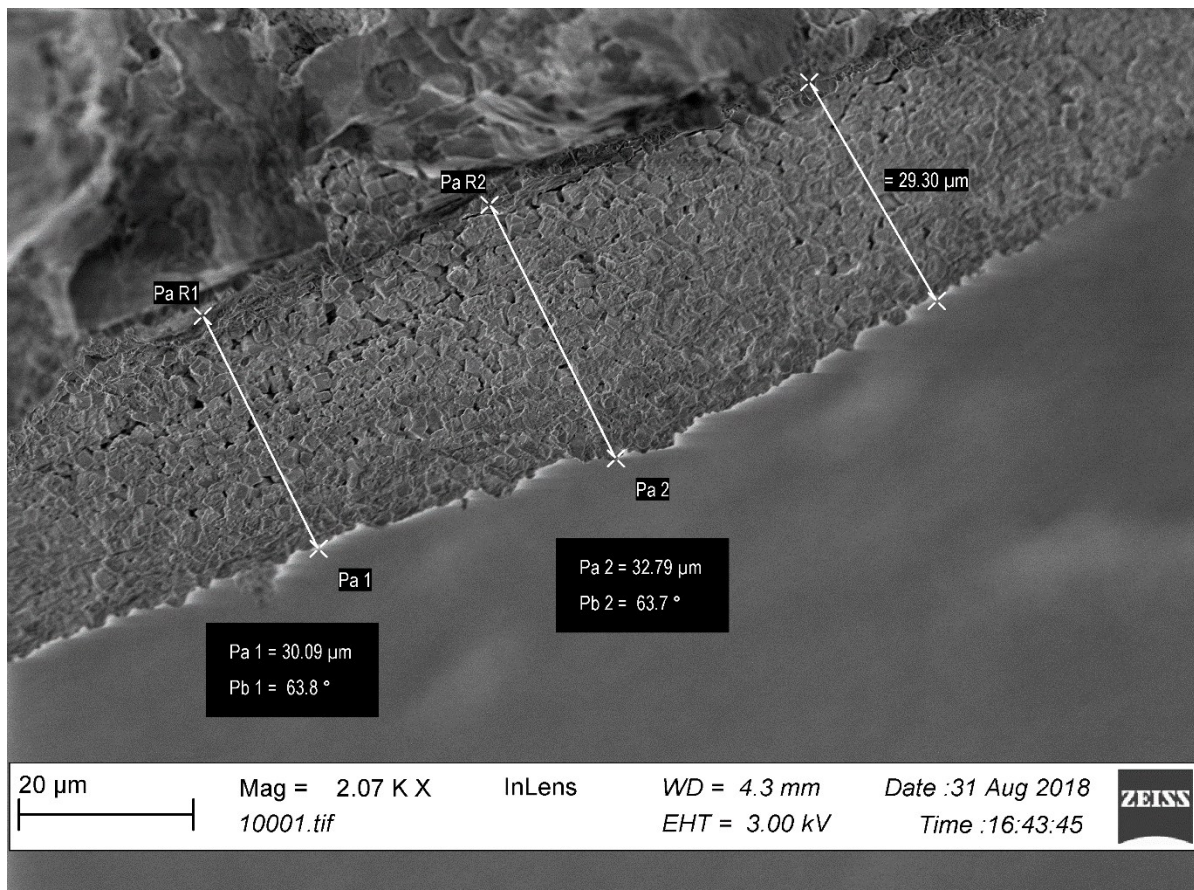


Figure S1. SEM micrograph representing washcoat thickness for single layer Cu-SSZ-13 sample with catalyst loading of 2.4 g/in³.

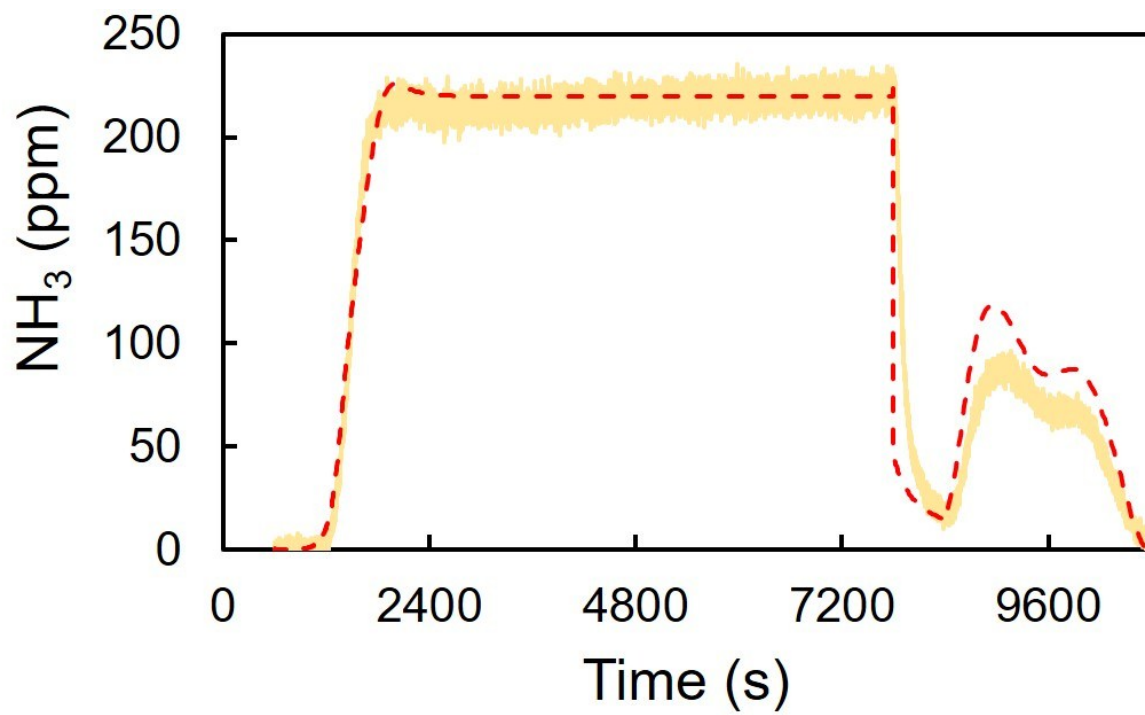


Figure S2. Transient NH₃ uptake and temperature programmed desorption as a function of time for Cu(2.1)_y sample using A_{1f} as 3.1e1 rather 2.7e1.

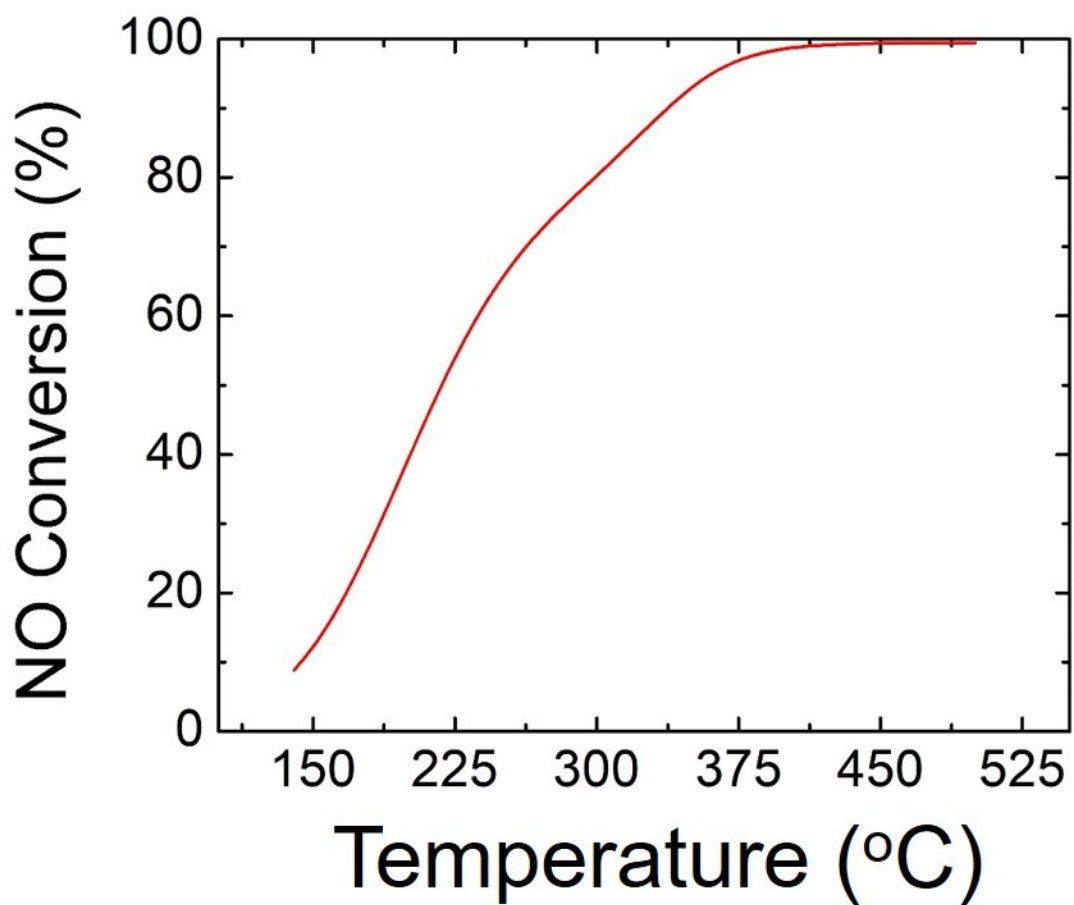


Figure S3. Model prediction of steady state NO conversion as a function of temperature (°C) using feed 500 ppm NH₃ and NO, 5% O₂ and balance Ar at 66k h⁻¹ while NH₃ oxidation steps (R3 and R4) are excluded from the overall reaction scheme.

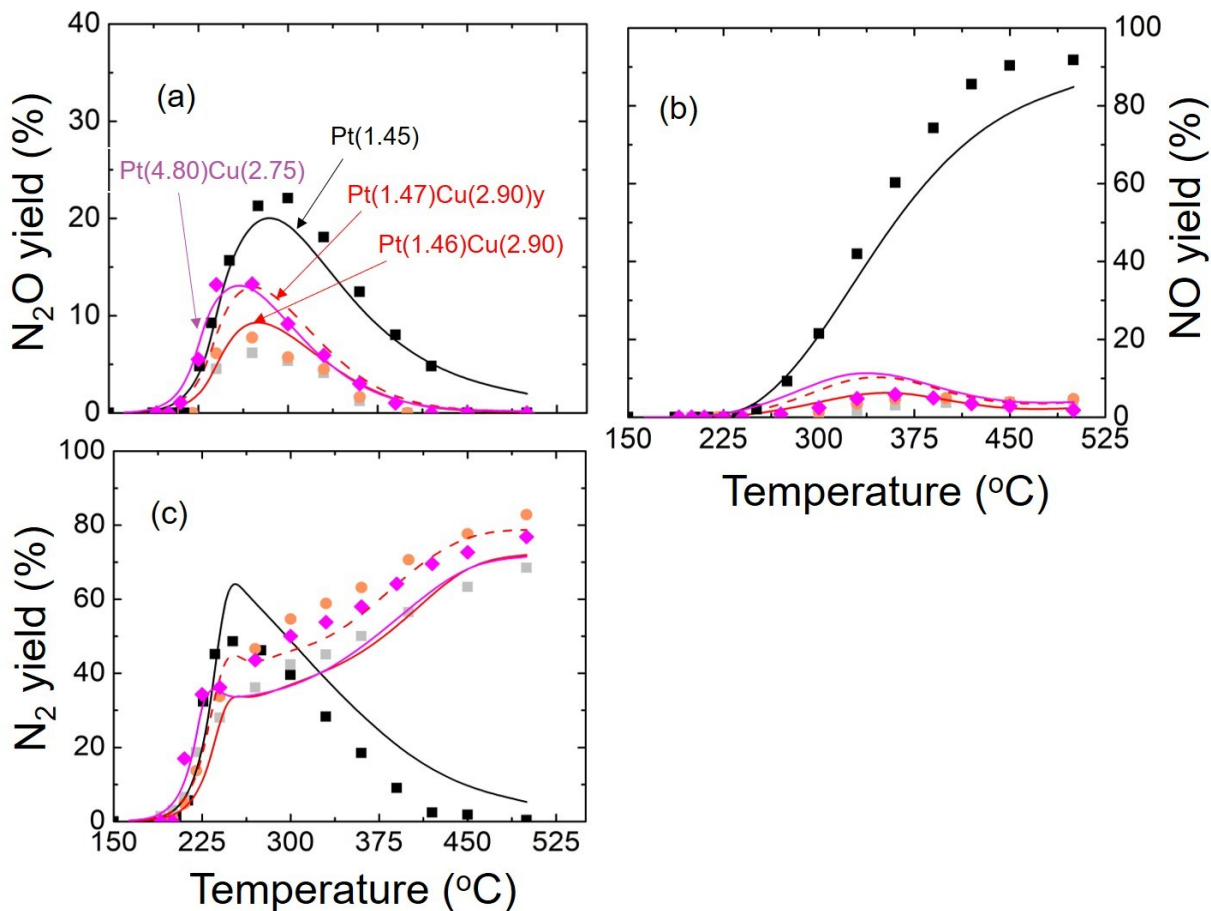


Figure S4. Steady state N₂O (a), NO (b) and N₂ (c) yield (%) as a function of temperature (°C) for differed samples. Feed: 500 ppm NH₃, 5% O₂ and balance Ar at 332k h⁻¹. Line represent simulation results and symbols represent experiments (dark square – Pt(1.45), light square – Pt(1.46)Cu(2.90), circle – Pt(1.47)Cu(2.90)y, diamond – Pt(4.80)Cu(2.75)).

Section S5.

A limited number of NO oxidation experiments were carried out and very low NO conversion was observed even in the absence of water. This finding is in line with previous results [1]. Metkar et al. [2] showed that NO oxidation on Cu-SSZ-13 is inhibited by the formed product NO₂ with the reaction rate negative order with respect to NO₂ [2, 3]. However, this surface-bound NO₂ is immediately removed through fast SCR with NH₃ present, enabling increased NO oxidation. To this end, a scheme that includes steps for NO oxidation and fast SCR cannot be ruled out. However, with our intent to minimize the number of reaction steps, these steps were not included. Also, the experimental results show negligible N₂O formation (< 10 ppm), hence N₂O formation steps are not included in the reaction scheme.

Experiment results including NH₃ TPD and SCR over a range of temperatures show evidence of at least two types of active sites for the Cu-SSZ-13 catalyst. Previous works have reported several active sites in Cu-SSZ-13, including Cu²⁺, [Cu(OH)]⁺, CuO and Brønsted acid sites, denoted by H⁺. We define the S1 site to represent the cupric cation in the form of Cu²⁺ and Cu(OH)⁺ species while the S2 site represents H⁺. Cu may also exist in the form of CuO clusters which are known to be active for NO oxidation but have negligible activity for SCR [1]. High temperature hydrothermal aging eliminates a significant fraction of the S2 sites; this is discussed in more detail in the next section.

The set of kinetic parameter pairs (A_r , E_r) were estimated by fitting integral conversion and kinetic data for unmodified sample Cu(2.1). Reaction steps R1 to R6 were deconvoluted by regulating input feed compositions to minimize the number of parameters to be estimated at once. First, the kinetic parameters for R1 and R2 were estimated using transient NH₃ uptake and TPD experimental data for a feed consisting of 200 ppm NH₃ and balance Ar. Then, keeping the R1 and R2 parameters fixed, the R3 and R4 kinetic parameter tuning was accomplished using steady state NH₃ oxidation experiment data comprising a feed of 500 ppm NH₃ and 5% O₂. Finally, the R1 through R4 parameters were fixed while R5 and R6 parameters were estimated through a fit of steady state SCR integral data and low temperature differential conversion data. The SCR reactor was validated by simulating results for the unmodified Cu(3.2) sample which differed only in terms of the washcoat thickness from Cu(2.1).

In addition to the SCR kinetic parameters, the ratio of the fluid and solid phase diffusivities, λ_{scr} ($D_{f,j}/D_{e,scr,j}$), is known to be confined within a finite range but must be estimated. The use of an effective diffusivity $D_{e,scr,j}$ for each reacting species assumes that the dominant transport is in the interstitial voids between the zeolite crystallites. The reported range of λ_{scr} values between 50 to 100, convey the variability of two key factors; namely, the crystallite size and washcoat properties, the former determined by the zeolite synthesis and any post-synthesis milling, and the latter by the washcoat deposition process.

To obtain a good estimate of the kinetic parameters and λ_{scr} an interactive regression method was adopted. The following approach relies on the fact that washcoat diffusion through the SCR layer is a critical rate-limiting process for the dual-layer ASC at high temperature ~300 °C. The first step involved SCR model tuning for single-layer monolith SCR data, confining λ_{scr} between 50 and 100. For each assumed λ_{scr} value the SCR data are fit, giving a unique set of kinetic parameters. Each set of parameters is then validated for an unmodified dual-layer ASC data set, specifically, Pt(1.46)Cu(2.90). The parameter set giving the best ASC data fit was selected.

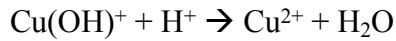
Section S6.

Previous researchers reported a standard SCR activation energy between 30 and 100 kJ/mol. Gao et al. [4] show the apparent SCR activation energy as a function of the Cu loading with low (<0.1 Cu/unit cell) and high (1-2 Cu/unit cell) exhibiting extremums of ~40 and 80 kJ/mol, respectively. Our catalyst composition had a Cu loading between 0.1 and 1 for Si/Al (12)

and Cu/Al (0.35). To this end, the apparent activation ~ 54 kJ/mol is consistent with the literature. The reaction order dependency of ~ 1 (NO) and ~ 0 (NH₃) over Cu- and Fe-zeolites has been reported by several researchers.

Section S7.

Fig. S8(a) shows that the second TPD peak at higher temperature associated with site S2 almost disappears with the aging treatment. Nevertheless, amount of NH₃ storage remains nearly the same as the pre-aged samples as a result of an enlargement of the S1 desorption peak. This phenomenon has been studied in detail by Luo et al. [5] and Gao et al. [6]. Gao et al. [6] explained that two NH₃ molecule adsorb on isolated Cu²⁺ while Cu(OH)⁺ and Brønsted (H⁺) sites bind one NH₃ molecule each. Hydrothermal aging treatment transforms Cu(OH)⁺ to Cu²⁺ by reacting with its neighboring Brønsted site (H⁺), forming water:



Now, as developed, site S1 represents isolated Cu²⁺ while S2 represents Brønsted (H⁺) and Cu(OH)⁺ species. The S2 site density, C_{S2} was reduced from 290 moles/(m³ washcoat) to ~ 90 moles/(m³ of washcoat) to achieve a satisfactory fit for the NH₃ TPD data while increasing C_{S1} from 600 to 700 moles/(m³ washcoat). Similarly, the kinetics for NH₃ oxidation and standard SCR were slightly modified to get a better fit. It is seen in Fig. S8(b) that NH₃ oxidation activity declines since the active site S2 is destroyed during the hydrothermal treatment. Post aging, the NH₃ oxidation rates (R3 and R4) reduce approximately to one-third of the pre-aged values. On the other hand, the NO conversion during standard SCR actually increases. The SCR rate R5 on the low temperature site S1 increases to ~ 1.75 times of the pre-aged R5 while R6 reduces to 0.03 times that of the pre-aged sample. The aged catalyst kinetic parameters are reported in Table 6. The low temperature NO conversion increases for both modified and unmodified samples. Finally, as before, the modified sample results were modeled using λ_{SCR} as 32 and modified R_{Ω2}. Unlike pre-aged samples, it is seen in Fig. 10d that effect of λ_{SCR} persists even at high temperature showing that the reaction remains in the mixed reaction + washcoat diffusion controlled regime.

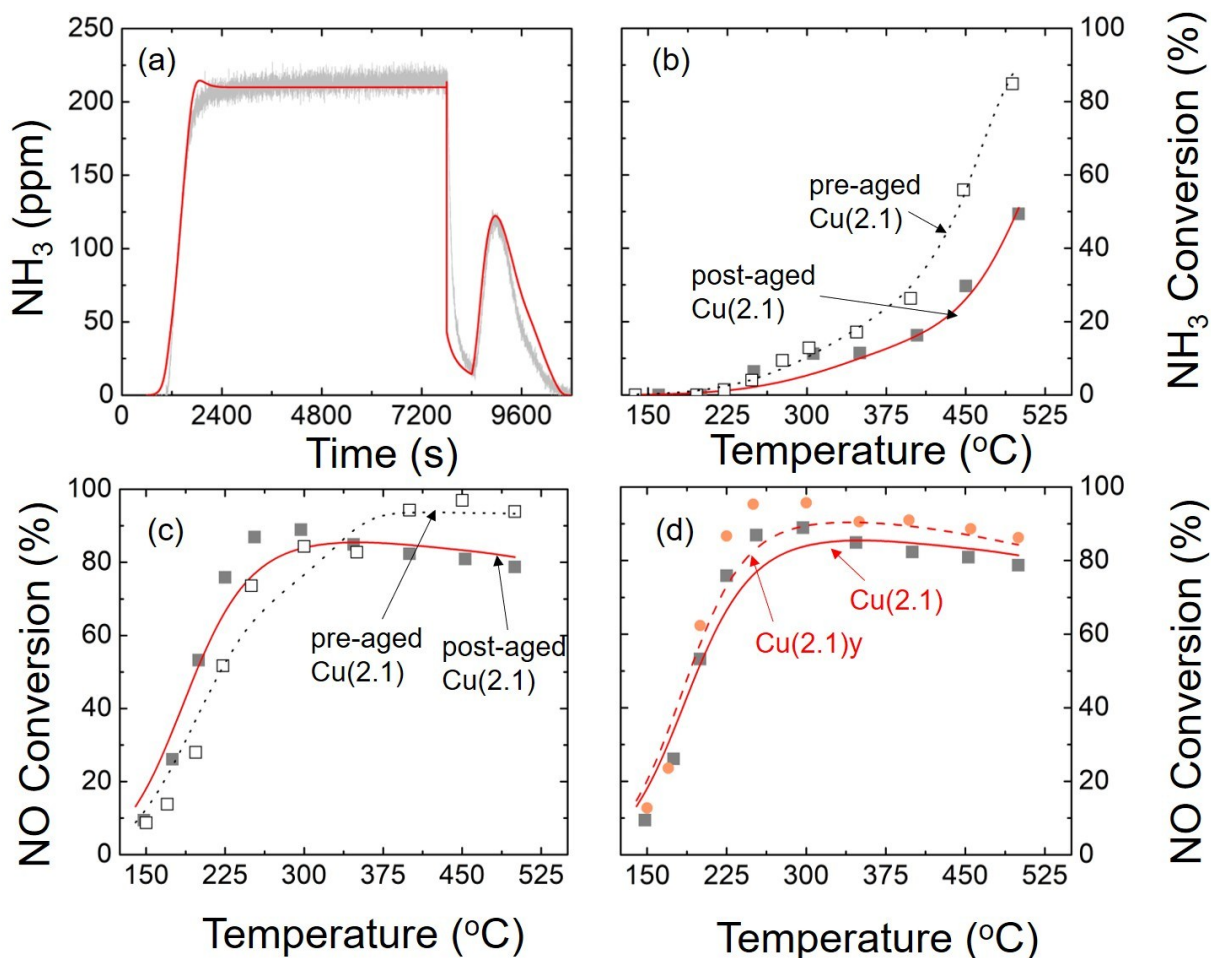


Figure S8. Experimental data (markers) and simulations (lines) results over hydrothermally aged Cu(2.1) sample (a-c). (a) Transient NH₃ adsorption and temperature programmed desorption as a function of time in seconds. (b) Steady state NH₃ conversion function of temperature with feed 500 ppm NH₃, 5% O₂ and balance Ar at 66k h⁻¹, pre-aged results are shown for comparison (c) Steady state NO conversion as a function of temperature with feed consisting 500 ppm of NH₃ and NO, 5% O₂ and balance Ar at 66k h⁻¹, pre-aged results are shown for comparison (d) Comparison performed for aged Cu(2.1) and Cu(2.1)y using SCR feed conditions. Lines represent simulation results and symbols represent experiments (light square – Cu(2.1), circle – Cu(2.1)y).

References:

[1] Verma, A. A., Bates, S. A., Anggara, T., Paolucci, C., Parekh, A. A., Kamasamudram, K., ... Ribeiro, F. H. (2014). NO oxidation: A probe reaction on Cu-SSZ-13. *Journal of Catalysis*, 312, 179–190. <https://doi.org/10.1016/j.jcat.2014.01.017>

- [2] Metkar, P. S., Balakotaiah, V., & Harold, M. P. (2012). Experimental and kinetic modeling study of NO oxidation: Comparison of Fe and Cu-zeolite catalysts. *Catalysis Today*, 184(1), 115–128. <https://doi.org/10.1016/j.cattod.2011.11.032>
- [3] Fahami, A. R., Nova, I., & Tronconi, E. (2017). A kinetic modeling study of NO oxidation over a commercial Cu-CHA SCR catalyst for diesel exhaust aftertreatment. *Catalysis Today*, 297, 10–16. <https://doi.org/10.1016/J.CATTOD.2017.05.098>
- [4] Gao, F., Mei, D., Wang, Y., Szanyi, J., & Peden, C. H. F. (2017). Selective Catalytic Reduction over Cu/SSZ-13: Linking Homo- and Heterogeneous Catalysis. *Journal of the American Chemical Society*, 139(13), 4935–4942
- [5] Luo, J., Kamasamudram, K., Currier, N., & Yezerets, A. (2018). NH₃-TPD method for quantifying the hydrothermal aging of Cu/SSZ-13 catalysts. *Chemical Engineering Science*, 190, 60–67. <https://doi.org/10.1016/j.ces.2018.06.015>
- [6] Gao, F., & Szanyi, J. (2018). On the hydrothermal stability of Cu/SSZ-13 SCR catalysts. *Applied Catalysis A: General*, 560(March), 185–194. <https://doi.org/10.1016/j.apcata.2018.04.040>